AD

CONTRACT REPORT ARBRL-CR-00405

CALCULATIONS OF THE PERFORMANCE OF EXPLOSIVE IMPULSE GENERATORS

Prepared by

Science Applications, Inc.
P. O. Box 2351
La Jolla, CA 92038

August 1979

US ARMY ARMAMENT RESEARCH AND DEVELOPMENT COMMAND
BALLISTIC RESEARCH LABORATORY
ABERDEEN PROVING GROUND, MARYLAND

Destroy this report when it is no longer needed.
Do not return it to the originator.

Secondary distribution of this report by originating or sponsoring activity is prohibited.

Additional copies of this report may be obtained from the National Technical Information Service, U.S. Department of Commerce, Springfield, Virginia 22161.

The findings in this report are not to be construed as an official Department of the Army position, unless so designated by other authorized documents.

The use of trade names or manufacturers' names in this report does not constitute indorsement of any commercial product.

UNCLASSIFIED

SECURITY CLASSIFICATION OF THIS PAGE *(When Data Entered)*

REPORT DOCUMENTATION PAGE		READ INSTRUCTIONS BEFORE COMPLETING FORM
1. REPORT NUMBER CONTRACT REPORT ARBRL-CR-00405	2. GOVT ACCESSION NO.	3. RECIPIENT'S CATALOG NUMBER
4. TITLE *(and Subtitle)* CALCULATIONS OF THE PERFORMANCE OF EXPLOSIVE IMPULSE GENERATORS		5. TYPE OF REPORT & PERIOD COVERED Final 6. PERFORMING ORG. REPORT NUMBER SAI-78-919-LJ
7. AUTHOR(s) M. W. McKay and R. N. Schlaug		8. CONTRACT OR GRANT NUMBER(s) DAAK11-78-C-0049
9. PERFORMING ORGANIZATION NAME AND ADDRESS Science Applications, Inc. P. O. Box 2351 La Jolla, CA 92038		10. PROGRAM ELEMENT, PROJECT, TASK AREA & WORK UNIT NUMBERS 8X363304D215 63304A
11. CONTROLLING OFFICE NAME AND ADDRESS US Army Ballistic Research Laboratory ATTN: DRDAR-BLB/Dr. Norman E. Banks Aberdeen Proving Ground, MD 21005		12. REPORT DATE AUGUST 1979 13. NUMBER OF PAGES 48
14. MONITORING AGENCY NAME & ADDRESS*(if different from Controlling Office)* US Army Ballistic Missile Defense Advanced Technology Center ATTN: ATC-M P. O. Box 1500 Huntsville, AL 35807		15. SECURITY CLASS. *(of this report)* UNCLASSIFIED 15a. DECLASSIFICATION/DOWNGRADING SCHEDULE

16. DISTRIBUTION STATEMENT *(of this Report)*

Approved for public release; distribution unlimited.

17. DISTRIBUTION STATEMENT *(of the abstract entered in Block 20, if different from Report)*

18. SUPPLEMENTARY NOTES

19. KEY WORDS *(Continue on reverse side if necessary and identify by block number)*

High Explosives	Stress Attenuation
Explosive Loading	Structural Response
Rocket Motors	Numerical Calculations
Shock Waves	

20. ABSTRACT *(Continue on reverse side if necessary and identify by block number)*

Numerical calculations of the performance of explosive impulse generators were performed. The explosive impulse generators were intended to provide the guidance thrust for a fast response missile guidance system. The objective of the calculations was to provide information to help determine whether an explosive impulse generator could be designed to produce the required impulse without generating a stress environment within the vehicle body that would cause damage either to the internal electronics or to the remaining undetonated impulse generators. Several 1D finite difference calculations were performed to analyze

DD FORM 1 JAN 73 1473 EDITION OF 1 NOV 65 IS OBSOLETE

UNCLASSIFIED

SECURITY CLASSIFICATION OF THIS PAGE *(When Data Entered)*

(Block 20)

various buffering or stress attentuation schemes while at the same time estimating the impulse generated by the explosive thruster systems. The 1D analyses show that it may be possible to design a system with the required features but further analysis involving 2D explosive loading/ structural response calculations is required.

FOREWORD

The objective of the research reported herein was to calculate the performance of explosive impulse generators as part of a study of the feasibility of an explosively driven missile guidance system. This research was conducted for the U. S. Army Ballistic Research Laboratory, Aberdeen, Maryland, under Contract DAAK11-78-C-0049. It was monitored by Dr. Norman E. Banks of BRL to whom the authors wish to express their appreciation for his interest and guidance. The authors would also like to thank Dr. Yong S. Park of BRL for reviewing this report. Finally, we would like to thank Ms. Gayle Wathen and Mrs. Peg Hubbard for preparing the manuscript.

TABLE OF CONTENTS

LIST OF TABLES

LIST OF FIGURES

1. INTRODUCTION

This report describes analyses done in support of a program to develop a missile guidance system which employs small explosive charges to provide the guidance thrust. Such a system would be capable of providing a considerably shorter response time than more conventional systems which use rocket motors.

The principal problem in designing such a system is to provide the impulse required to maneuver the vehicle without generating a stress environment within the vehicle body that would cause damage either to internal electronics or to remaining undetonated impulse generators. The work described in this report addresses this problem. In particular, methods of minimizing the peak loads on the vehicle were investigated using a series of 1D finite difference calculations. Some promising techniques were identified. In addition, charge size requirements for producing the desired impulse were analyzed and some preliminary designs were identified for further study in a subsequent phase of the program.

2. HE IMPULSE GENERATOR DESIGN CONCEPT

The general configuration for the HE thruster system being considered is shown in Figure 1. Thrust is provided by pairs of charges located on the surface of the vehicle body as shown. In the system investigated here, these charges are located in grooves approximately four inches long and 3/4-inch wide with a roughly semicircular cross-section. (In other studies, other thruster shapes are being investigated.) A total of sixteen pairs of thrusters are required; each must be capable of generating sufficient impulse to provide a change in the vehicle velocity of 30 feet/second. Therefore each thruster must be capable of producing a velocity change of 15 feet/second. The nominal weight of the vehicle is twenty-four pounds so the impulse required from each thruster is 11.2 pound-second or in cgs units 5.0×10^6 dynes-second.

The general configuration of the explosive impulse generator is shown in cross-section in Figure 2. The explosive charge is PETN and is located on the lower surface of a tungsten plate. The plate provides confinement for the charge after detonation and thereby increases the impulse produced per unit charge mass. Tungsten is used because of its high density. The cavity in the vehicle body shown here is semicircular in cross-section with about a 3/8-inch radius. However, the dimensions and shape are considered variables in the study, within obvious limits. The length of the cavity is four inches. For purposes of this study the vehicle was considered to be titanium, although other materials are being considered in other studies.

In the intervening space between the explosive charge and the vehicle a variety of buffer materials have been considered in an attempt to reduce the peak stress loading on the vehicle body. An air gap, shock absorbing foam, layers of materials with differing shock impedances as well as various combinations of these have been investigated. These are discussed in the next section.

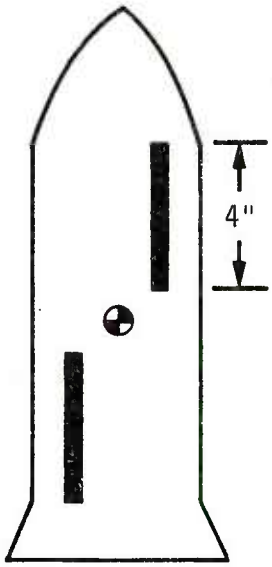

Figure 1a. Location of Pair of Impulse Generators.

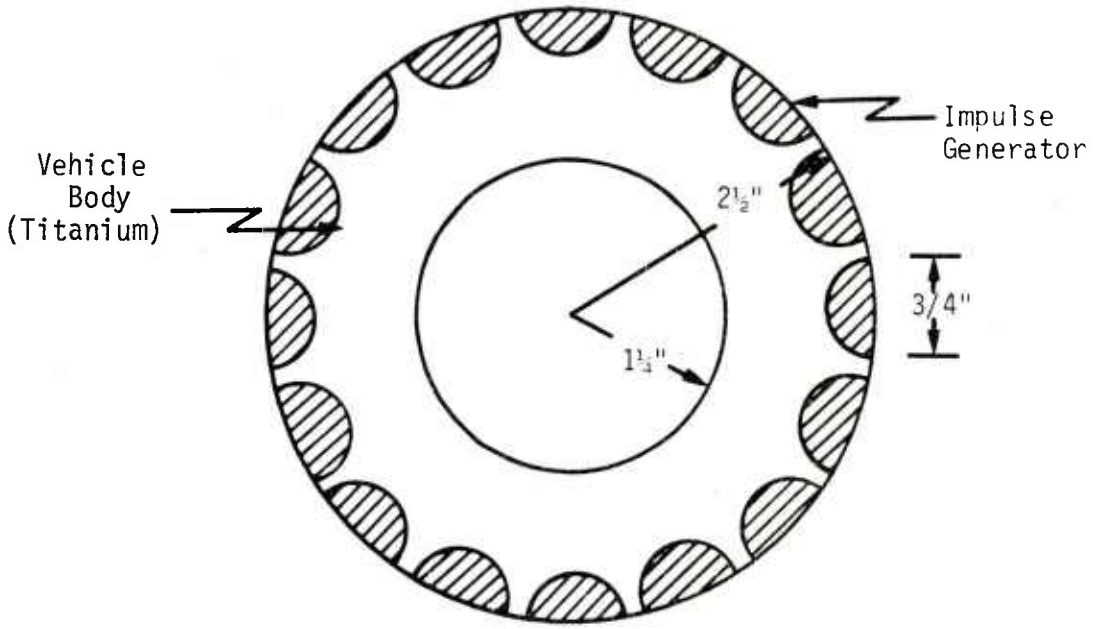

Figure 1b. Cross Section of Vehicle Body.

Figure 1. Impulse Generator Concept.

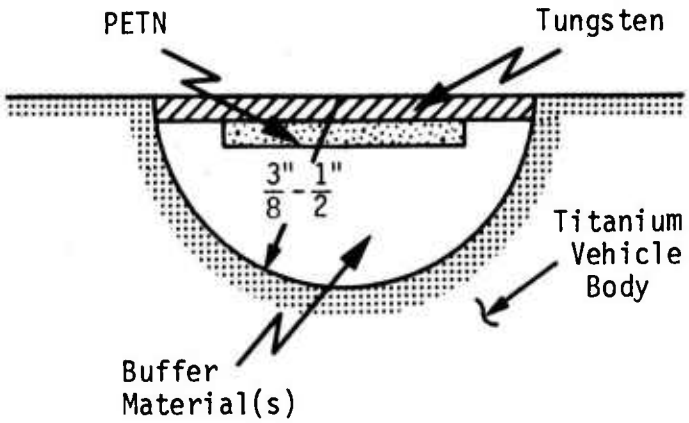

Figure 2. Typical Configuration of Explosive Impulse Generator.

3. STRESS ATTENUATION METHODS

The detonation pressure of PETN is about 335 kilobars. Since this stress level would cause substantial damage to the vehicle body it is necessary to provide some type of buffer to reduce the peak stress. Three methods have been investigated in this study:

1. shock absorbing foam
2. air gap
3. impedance mismatched layers.

The significant features of all of these will be discussed below.

3.1 METAL FOAMS

The shock attenuating properties of foams are well known and have been used in the past for a variety of explosive loading applications. In one particularly pertinent example, a neoprene rubber foam was used to attenuate the shock wave produced by detonating EL-506K sheet explosive.[1] In this case the explosive was being used for structural testing of re-entry vehicles. However, since the detonation pressure of the explosive was considerably higher than the peak stress of the load being simulated, it was necessary to attenuate the peak pressure while still providing the required total impulse.

Figure 3 shows the peak stress attenuation produced as a function of foam thickness. Although this figure shows a lower stress range than we are interested in, we can see that a foam-to-explosive thickness ratio of about 50 is required to attenuate the peak stress to 10 kbar. Because of space limitations in the HE thruster, the largest possible foam-to-explosive thickness ratio would be about ten. This means that to achieve the desired stress attenuation (nominally down to 10 kbar) a foam providing more attenuation is required for our application.

---

1. G. R. Abrahamson, "Explosively Induced Impulses," Int. Report No. 009-62, Stanford Research Institute, Menlo Park, California, July 20, 1962.

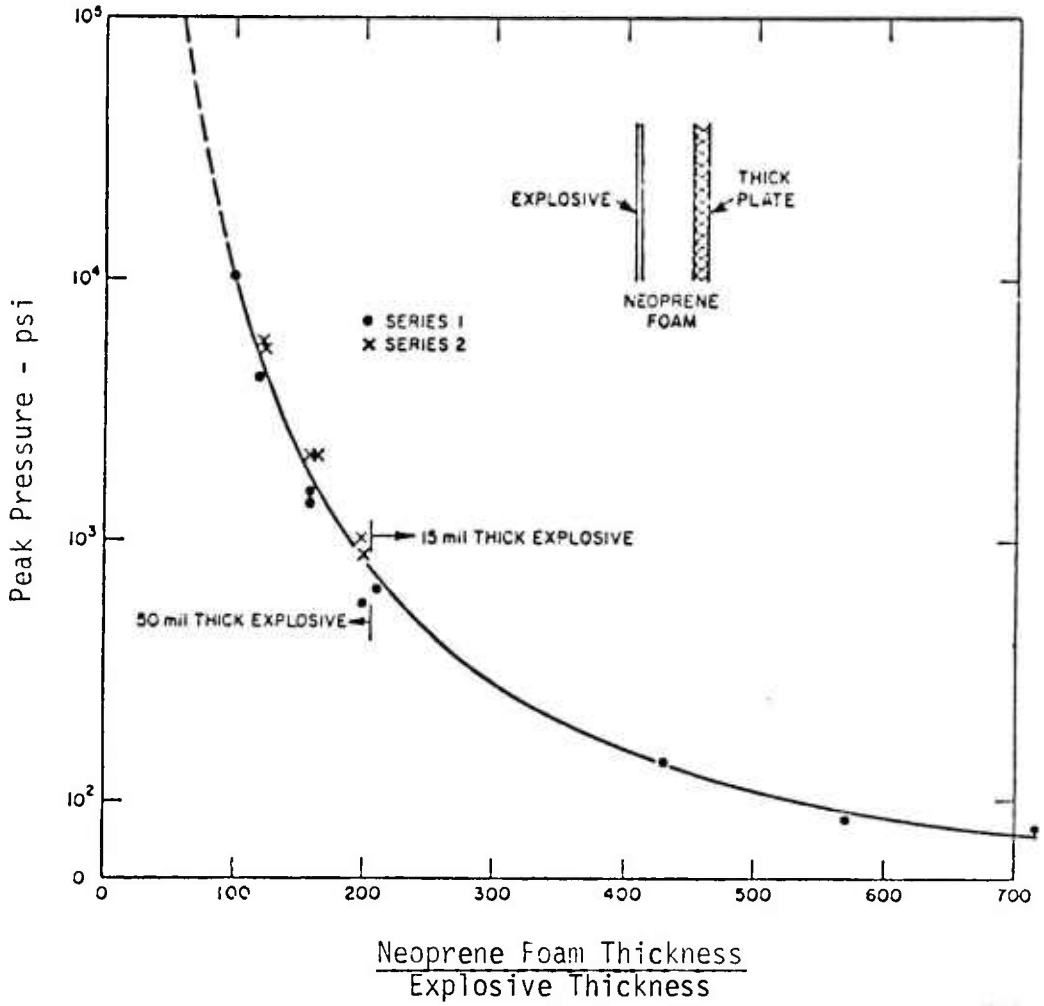

Figure 3. Peak Stress Attenuation Produced by Neoprene Rubber Foam (reproduced from Reference 2).

The shock attenuation properties of a foam depend primarily on two variables, the porosity and the crush strength; increasing either parameter results in more energy from the high pressure part of the stress wave being expended in compressing the voids. It turns out that metal foams have a fairly high crush strength while still having fairly high porosity, so we decided to investigate their effect in the HE thruster system.

We chose to investigate an aluminum foam that is described in Reference 2. It has an initial density of 1.93 gm/cm^3 and a fully crushed density of 2.7 gm/cm^3 (the normal density for aluminum) for a distention ratio of 1.4. Figure 4 shows hydrosataic loading and unloading curves for the idealized equation-of-state we used to describe this material. On initial loading the material begins to crush at .5 kbar and is fully crushed at 5 kbar. For peak loads between those two levels the material is partially crushed and releases to some intermediate density when unloaded. It should be noted that in constructing this equation-of-state no attempt was made to fit details of experimental data for loading and unloading of metal foams. Rather, the equation-of-state was intended to reproduce the general properties of this type of material, assuming certain physically realistic values for distention ratio, crush strength, etc. Details of the computerized model used for this equation-of-state, including the high pressure, energy dependent part that we have not discussed here, can be found in Reference 3. This model was patterned after the Tillotson equation-of-state for metals described in Reference 4. The high pressure properties for solid aluminum given in this reference were used in this model to describe the behavior of the fully compacted state.

Results of calculations using this material will be presented in Section 4.

---

2. W. Herrmann, "Equation of State of Crushable Distended Materials," SC-RR-66-2678, Sandia Laboratory, Albuquerque, New Mexico, March 1968.

3. D. E. Maxwell, "Improved TAM Equation of State," TCAM Technical Memo 72-1, Physics International Company, San Leandro, California, 1972.

4. J. H. Tillotson, "Metallic Equations of State for Hypervelocity Impact," GA-3216, General Atomic, La Jolla, California, July 1962.

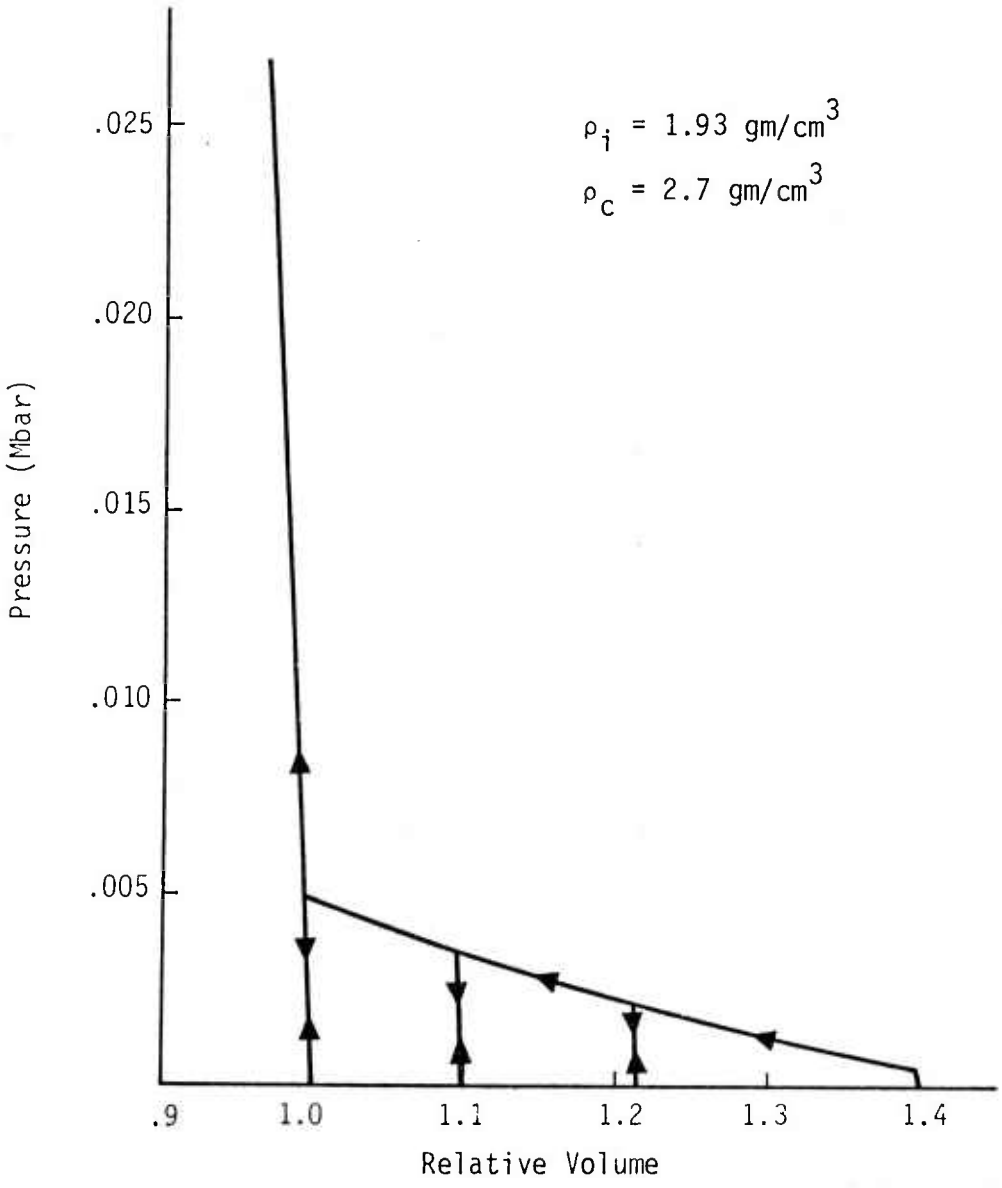

Figure 4. Low Pressure Hydrostat for Distended Aluminum.

3.2 AIR GAP

As we said earlier, the shock attenuating ability of a foam increases with increasing porosity. Carrying this to the extreme, the maximum porosity is no foam at all but rather a void or an air gap. We would expect that the peak stress in the vehicle body would be substantially reduced over the detonation pressure by separating the explosive from the body by a sizeable air gap. In this case the detonation products would expand from the detonating charge, fill the gap, and stagnate against the vehicle body. This stagnation will produce a considerably higher pressure at the interface than if the detonation products had expanded quasi-statically, but that pressure should still be much lower than the detonation pressure.

The lower limit for such a pressure is the pressure for a quasi-static expansion. To get a rough idea of the magnitude of this lower limit (primarily to see if it was unacceptably high) we calculated the quasi-static expansion for a configuration approximately as shown in Figure 2. Using the JWL equation-of-state for PETN,[5] this turns out to be about 3 kbar. Thus we can expect the stagnation pressure to be considerably higher than that.

Several calculations involving an air gap are presented in Section 4. In turns out that for the configuration in Figure 2 (3/8-inch radius cavity, .04-inch thick flyer plate and explosive charge, 1/2-inch wide charge) the stagnation pressure is about 60 kbar, which is higher than we would like. However, this stagnation pressure is independent of the solid material at the interface (since the shock impedance mismatch is essentially infinite), so by lining the cavity with the proper materials we can take advantage of some of the properties of shock waves propagating through impedance-mismatched materials to reduce this stress further. This is discussed in the next section.

5. E. L. Lee, et al., "Adiabatic Expansion of High Explosive Detonation Products," UCRL-50422, Lawrence Radiation Laboratory, Livermore, California, May 2, 1968.

FOR 2 MATERIALS

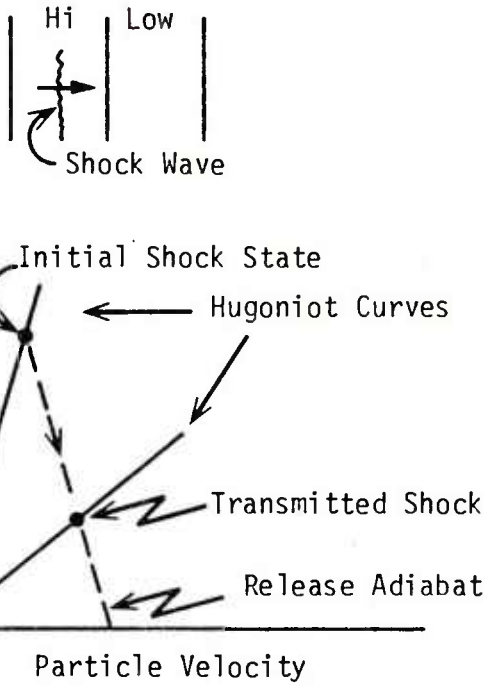

FOR 3 MATERIALS

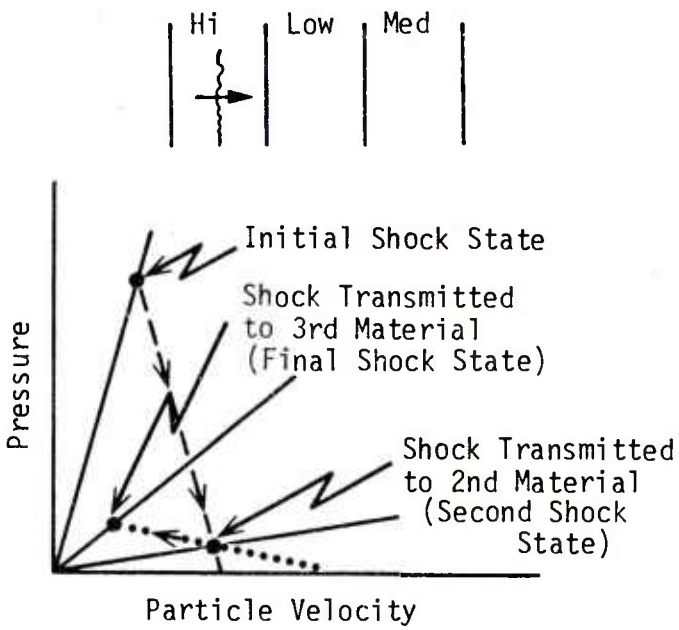

Figure 5. Effects of Impedance Mismatching.

3.3 EFFECTS OF SHOCK IMPEDANCE MISMATCHING

If materials with widely differing shock impedances are combined properly, a shock wave propagating through them can be substantially reduced in magnitude. The mechanism for this is shown graphically in Figure 5. The case of two materials is shown first. In this case a shock wave in the higher impedance material is transmitted to a lower impedance one. The Hugoniot curves for these materials are shown in pressure-particle velocity space, with the higher impedance material having the higher slope. When the initial shock wave reflects from the interface, a rarefaction propagates back into the first material, and a lower pressure shock wave is transmitted into the second material. The state of the material in the rarefaction region is described by an adiabat through the initial state (shown dashed), and the magnitude of the transmitted shock wave is determined graphically by the intersection of that adiabat with the Hugoniot for the second material.

In the case of three materials arranged as shown in Figure 5, the stress can be reduced even further. The three materials are designated as high impedance, low impedance and intermediate impedance, and the shock wave propagates through them in that order. As was demonstrated for the case of two materials, the magnitude of the shock wave transmitted to the low impedance material is determined by the intersection of the release adiabat for the first material with the Hugoniot curve for the second. This is labeled as the second shock state in Figure 5. When this second shock reflects from the interface between the low and intermediate impedance materials, the pressure increases as a rear-facing shock is reflected back into the middle material and a shock wave is transmitted into the third material. The state of the material in the region of the reflected (rear-facing) shock is represented by a Hugoniot curve for the low pressure material. This Hugoniot curve has the second shock state as its initial state; furthermore, because the reflected shock is a rear-facing or stopping shock, the slope of the Hugoniot curve is negative on the pressure-particle velocity diagram. This curve is shown dotted in Figure 5. The final shock state is then determined by the intersection of that reflected shock Hugoniot for the second material with the normal Hugoniot for the third.

If, for example, in the two material case the first material is tungsten and the second is the titanium vehicle body, a substantial reduction in the pressure transmitted to the vehicle occurs. If for the three material case we insert a low impedance material such as lexan or some other plastic between the tungsten and the titanium, the stress is reduced even further. As we said earlier, the stagnation pressure of the expanding detonation products is independent of the material at the interface. Therefore by lining the cavity with tungsten and lexan, it appears that we can reduce the stress substantially below the stagnation pressure.

The actual situation is not quite as straightforward as described above. The analysis presented pertains only to the first shock transmitted through the materials. Following this first transmission there are subsequent reflections within the layers that serve to increase the transmitted stress. If the incident stress wave is a step function, the transmitted wave will eventually "ring up" to the peak incident stress and the net effect will be to round off the front of the transmitted wave. If, however, the incident stress wave decays behind the peak, the peak transmitted stress will be lower. The layered materials effectively cause a dispersion of the wave, removing the high frequency part in the peak of the wave and spreading the transmitted impulse out over a longer time. The amount of this dispersion and, hence, the reduction in the peak stress, depends on the thickness of the layers and the width of the incident stress pulse.

The only way to effectively analyze this phenomenon is through numerical computations. Such calculations for a variety of configurations employing impedance mismatched layers are presented in Section 4.

4. 1D FINITE DIFFERENCE CALCULATIONS OF THE STRESS ENVIRONMENT

All finite difference calculations done in this program were performed using the STEALTH codes.[6] These are 1D and 2D Lagrangian finite difference codes modeled after the HEMP family of codes[7] currently in use at the Lawrence Livermore Laboratory. The codes have a broad range of capabilities for problems involving the dynamics of fluid and solid continua. They contain a full range of material property models including elastic-plastic flow, compaction of porous solids and high explosive detonation routines. In addition, the 2D codes contain both slideline and rezone capabilities which are often required for explosive/solid interaction problems such as the ones under consideration here.

As a first step toward evaluating the stress environment produced by the candidate HE thruster designs and to analyze the effectiveness of the various buffering schemes mentioned in the previous sections, a series of 1D calculations was done. In these calculations the one-dimensional motion along a line through the center of the cavity is calculated as if all materials were infinite slabs. This is a fair approximation for motions along the axis of symmetry but poorly approximates the motions in other regions where 2D effects are more important. Because they are inexpensive and can be run quickly, however, these calculations provide an effective method to compare the relative effects of a wide variety of configurations in a short time.

In the first series of calculations several things were investigated:

1. The effect of aluminum foam in attenuating the shock wave from the HE detonation;
2. The effect of an air gap in reducing the stress; and
3. The need for a flyer plate confining the explosive charge in order to reduce the total quantity of explosive required.

---

6. "STEALTH - A Lagrange Explicit Finite-Difference Code for Solids, Structural and Thermohydraulic Analysis," Volume 1-4, EPRI NP-260, Electric Power Research Institute, Palo Alto, California, August 1976.

7. M. L. Wilkins, "Calculation of Elastic-Plastic Flow," UCRL-7322, Rev. I, Lawrence Radiation Laboratory, Livermore, California, April 19, 1973.

The configurations analyzed in the first series of calculations are shown in Figure 6 along with the peak stress calculated at the titanium interface. In all cases the cavity depth is 3/8-inch. In the first three the flyer plate and PETN thicknesses are 0.041 and 0.044 inches respectively while in Calculation 4 the PETN thickness is .167 inches. This charge thickness is designed to produce the same total impulse as the PETN/tungsten configuration in the other three calculations.

Calculation 3 provides an estimate of the stress at the titanium interface when a non-attenuative material is used in the cavity. This is to be compared with Calculation 1 in which the porous aluminum foam discussed in Section 3.1 was used. The calculations show a significant stress reduction for the foamed aluminum although it is probably necessary to reduce the stress even further to avoid damage to the vehicle body.

From Calculation 2 we see that an air gap is even more effective in reducing the stress than the aluminum foam. However, the stress reduction is not sufficient in this case either.

From Calculation 4 we see that by eliminating the flyer plate and compensating by increasing the charge thickness, a substantially higher stress results. This demonstrates the need to use a flyer plate to maximize the impulse per unit mass of explosive and thereby minimize the total charge size.

The next series of 1D calculations investigated the combined effect of an air gap and foamed aluminum and also analyzed the effect of a high impedance layer at the titanium interface. The two configurations are shown in Figure 7. The dimensions for these configurations and the ones for the next series of calculations (Figure 8) were the same as for the previous series except for the noted exceptions.

The results of these calculations showed that the combined air gap/foamed aluminum was less effective in reducing the stress than either one used alone. However, the high impedance material at the interface

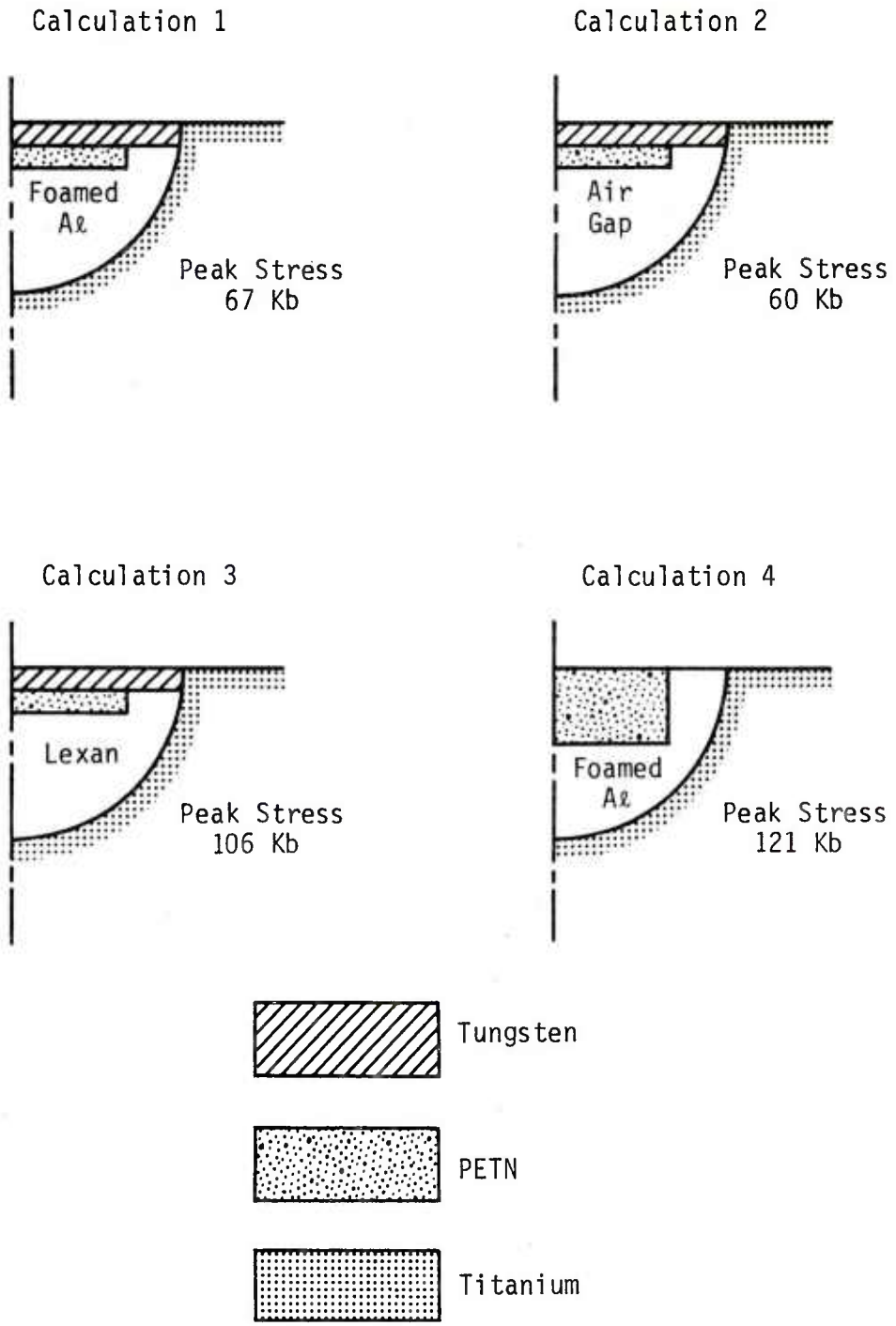

Figure 6. Configurations for 1D Calculations.

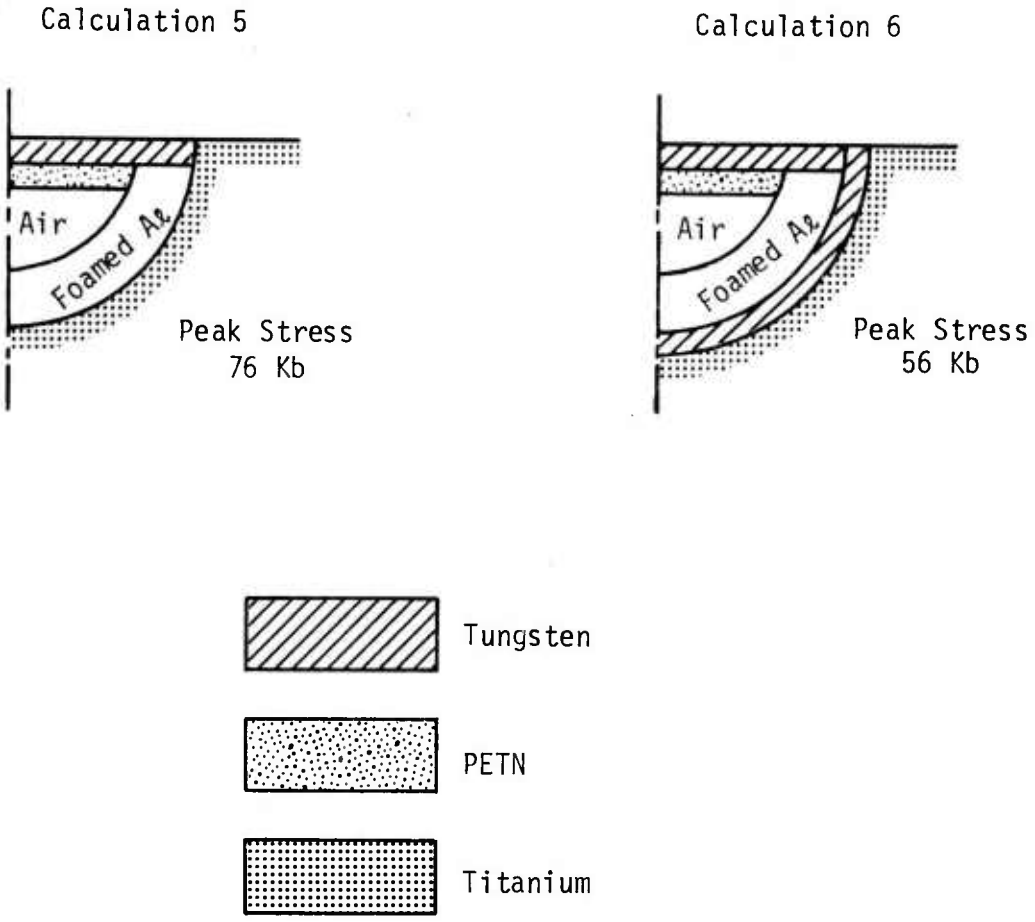

Figure 7. Configurations for 1D Calculations.

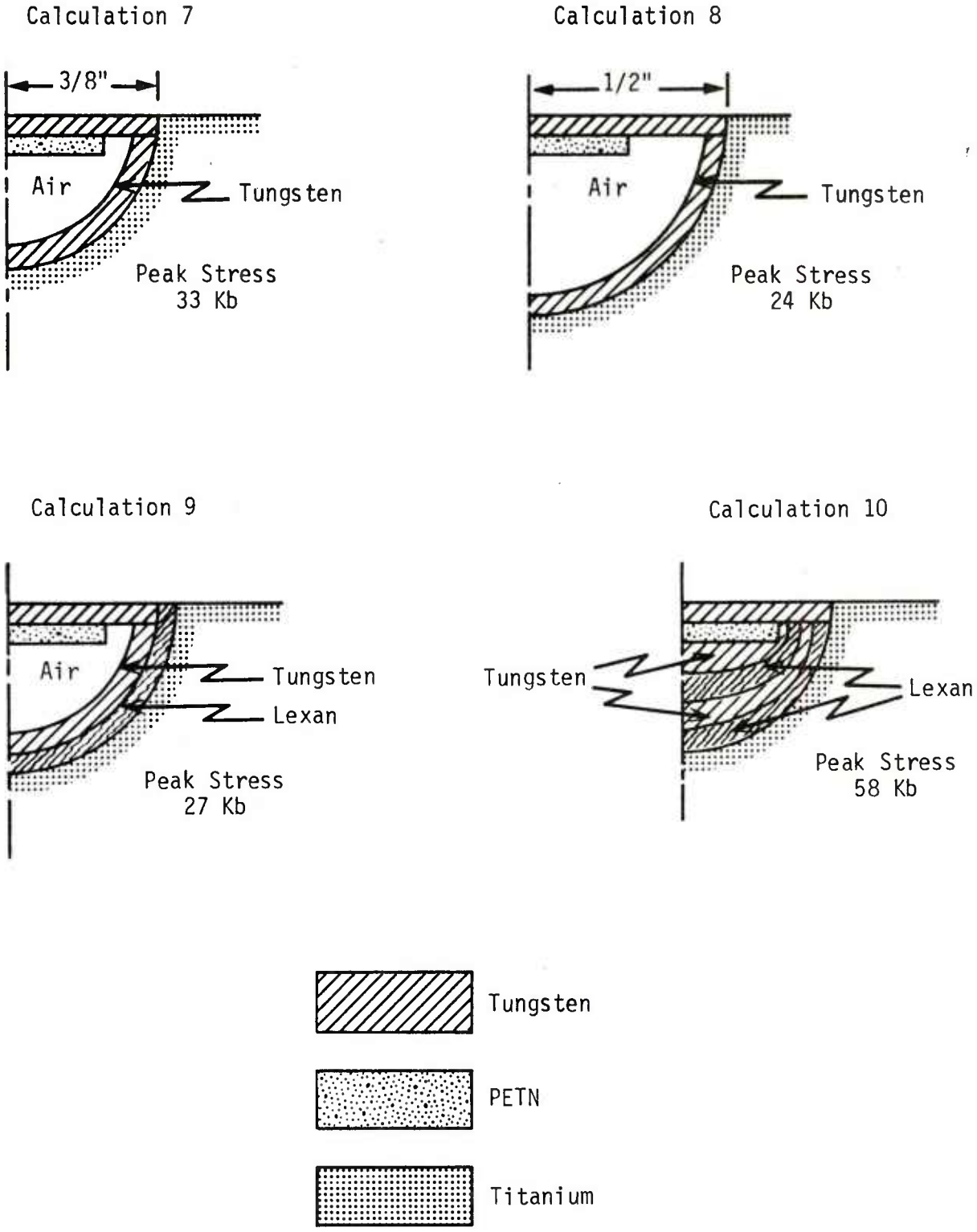

Figure 8. Configurations for 1D Calculations.

reduced the stress by 20 kbar for reasons discussed in Section 3.3. The overall reduction was still not sufficient, however.

We concluded from the first two series of calculations that the air gap provides the best means of attenuating the stress wave. Next we began to investigate methods to reduce that stress even further using impedance mismatched layers as discussed previously. The next series of four calculations, shown in Figure 8, was intended to analyze those methods.

Calculation 7 shows that a high impedance layer reduces the stress significantly (as compared with Calculation 2 - Figure 6). Comparing Calculations 7 and 8 shows that increasing the cavity size from 3/8 inch to 1/2 inch reduces the stress, as one would expect, but the magnitude of the reduction is not as impressive as we had hoped. The 1/2-inch size is about the upper limit on the radial extent of the cavity considering the location of the adjacent thrusters. However, it is possible to make the cavity somewhat deeper.

Calculation 9 shows the effect of impedance mismatched layers (in the three material configuration discussed in Section 3.3). This calculation is directly comparable with Calculation 7, and we see that a relatively modest stress reduction results.

The effect of multiple layers of impedance mismatched materials without an air gap was evaluated in Calculation 10. The result of this calculation demonstrates the importance of the air gap.

The primary objective of this group of 1D calculations was to determine the best methods for reducing the peak stress in the titanium missile body. From them we have identified an air gap with impedance mismatched layers at the cavity interface as a promising buffering scheme. At the same time these calculations provided an estimate for the impulse that would be produced by a given thruster design (although 2D effects are ignored). The results showed that the impulse for the charge/flyer plate thickness used in these designs is substantially lower than the

target value discussed in Section 2. A design utilizing a larger charge is required. This is discussed further in Section 5.

5. 1D IMPULSE CALCULATIONS

A first approximation to the impulse produced by a charge/flyer plate combination can be obtained from an approximate analysis. It has been shown that the Gurney formulas, which can be derived from the principles of conservation of energy and momentum using a few simple assumptions, provide a reasonable approximation to this impulse.[1,8] The first gives the momentum delivered to a flyer plate by an explosive charge in contact with the plate and with a free surface on the other side. This formula is

$$I_f = \sqrt{2E}\,\frac{m}{c}\left[\frac{3}{1 + 5\,\frac{m}{c} + 4\,\frac{m^2}{c^2}}\right]^{-\frac{1}{2}} \qquad (1)$$

where

I_f = momentum of the plate per unit mass of explosive,

m = mass of the plate,

c = mass of the explosive charge,

$\sqrt{2E}$ = the "Gurney constant" where E is approximately the heat of detonation of the explosive.

The second formula gives the momentum of a flyer plate and the detonation products when the rear surface of the explosive is confined rather than free. This formula is

$$I_c = \sqrt{2E}\left(\frac{m}{c} + \frac{1}{2}\right)\left[\frac{3}{1 + 3\,\frac{m}{c}}\right]^{-\frac{1}{2}} . \qquad (2)$$

In the second case, I_c would be equivalent to the impulse delivered to the vehicle if the charge was fully confined, i.e., no air gap. If an air gap is present the detonation products can expand freely initially so that momentum of the flyer plate is initially given by Equation (1).

---

8. I. G. Henry, "The Gurney Formula and Related Approximations for High-Explosive Deployment of Fragments," Report No. PUB-189, Hughes Aircraft Company, April 1967.

However, as the detonation products stagnate the momentum delivered to the flyer plate increases above that value. It is conceivable that eventually the momentum of the flyer plate and the detonation products, and therefore the momentum delivered to the vehicle, would reach the value predicted by Equation (2); however, this is unlikely. First of all, the "Gurney constant", $\sqrt{2E}$, is a measure of how much of the explosive energy can be converted into kinetic energy. In this case this constant will be somewhat below the ideal value given by assuming that E is equal to the heat of detonation. Secondly, considering 2D effects, the flyer plate will probably be accelerated out of the groove allowing venting of the detonation products before all the impulse is delivered. This effect cannot be evaluated in this 1D analysis. In any event we expect the final impulse for the cases involving an air gap to fall somewhere between the values predicted by the two formulas.

As we said in Section 2, the impulse required to produce a 15 foot/second velocity change in a 24 pound vehicle is 11.2 pounds-second or 5.0×10^6 dynes-second. It is interesting to use the two approximate formulas to calculate the various charge/flyer plate combinations capable of producing that impulse. For purposes of this analysis we have assumed that the flyer plate is tungsten with $\rho_o = 19$ gm/cm^3 and the explosive is PETN with $\rho_o = 1.77$ gm/cm^3 and $E_o = 5.71 \times 10^{10}$ ergs/gm. The various flyer plate/charge thicknesses are given in Table 1.

The designs calculated in the 1D calculations described in Section 3 had a flyer plate mass to charge mass ratio of 10. Since the flyer plate and charge thicknesses were .041 and .044 inches, respectively, we see from Table 1 that the Gurney formulas would predict that those designs would not produce sufficient impulse. This was supported by the 1D calculations.

Using what we have learned about stress attenuation methods from the first group of calculations and using the Gurney formulas to estimate the size requirements for the PETN/flyer plate combination, the

Table 1. Various Flyer Plate/Charge Thickness Combinations to Meet Required Thruster Impulse.

m/c	Equation (1) (unconfined)		Equation (2) (confined)	
	Flyer Plate Thickness*	Charge Thickness*	Flyer Plate Thickness*	Charge Thickness*
0	N/A	N/A	0	.196
1	.029	.310	.012	.131
5	.102	.220	.033	.071
10	.194	.208	.048	.052
20	.376	.202	.069	.037

* Dimensions are in inches.

design shown in Figure 9 was developed. For this design Equation (1) (unconfined case) predicts $I_f = 1.3 \times 10^6$ dynes-second while Equation (2) (confined case) predicts 6.22×10^6 dynes-second. This is to be compared with the design impulse of 5×10^6 dynes second. Since the design contains an air gap we expect the impulse produced to fall somewhere between the value predicted by the two equations.

Although a 2D calculation is required to determine the actual impulse produced (in order to account for the 2D effects in the equilibration of the detonation products within the cavity and venting of the products after the flyer plate leaves the cavity), useful information can be obtained from a 1D calculation. Therefore a 1D calculation was performed for this design in order to estimate both the peak stress at the titanium interface and the time history of the impulse generation.

The peak stress predicted for this new design was 41 kbar. This should be compared with 27 kbar for Calculation 9 which had a similar configuration but had a smaller charge and a correspondingly smaller air gap. Since the air gap was scaled to correspond with the thicker HE charge, it is logical to expect the peak stress to be the same. However, the thickness of the tungsten/lexan liner was not changed. Since the stress wave for the new design is broader because of the increased charge size, the liner is less effective in reducing the stress. To achieve the same attenuation it appears that the liner should have been scaled up also. The effect of varying the liner thickness on the attenuation of the stress pulse was not studied in the first phase of the program but should be studied in the future to optimize the effectiveness of the buffer system.

The impulse generation predicted for this new design is shown in Figure 10. The momenta in the flyer plate and detonation products are shown separately, as is the resultant impulse imparted to the vehicle. By conservation of momentum the three curves should sum to zero. Positive momentum is in the upward direction as shown in Figure 9 so that the vehicle momentum will be negative.

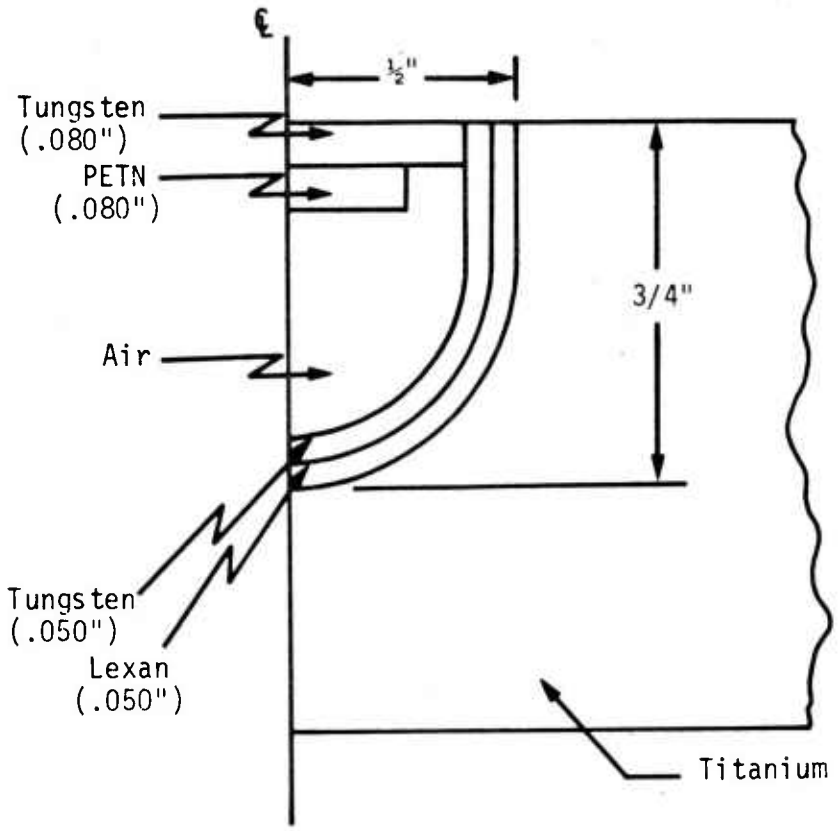

Figure 9. Revised Design for Increased Impulse.

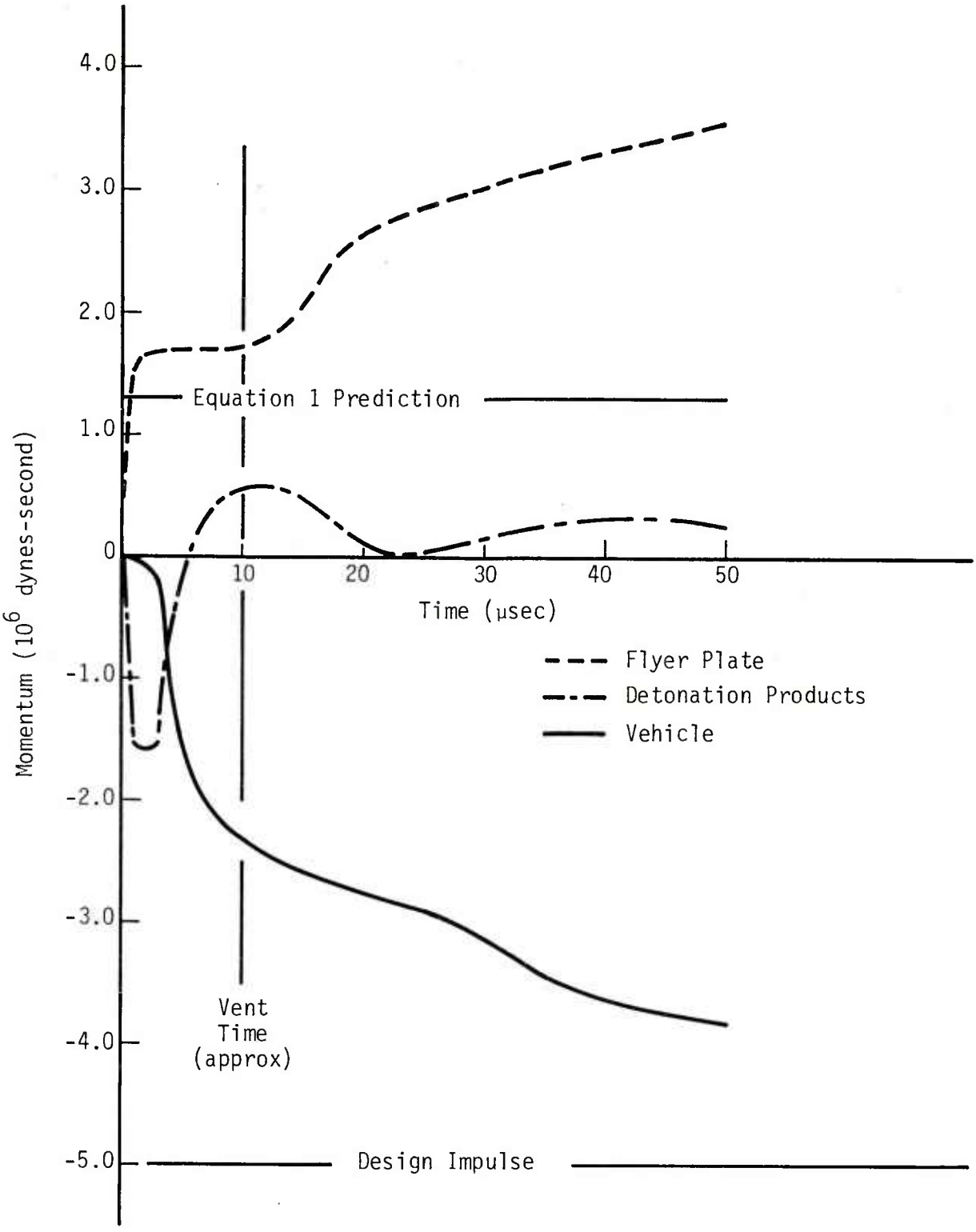

Figure 10. 1D Impulse Predictions.

We see that initially the flyer plate momentum reaches a value just above that predicted by Equation (1). At the same time the momentum in the detonation products is approximately equal and opposite. This is what we had predicted in our earlier discussion. At about 2 μsec the detonation products begin to stagnate at the cavity interface. At this point the momentum in the vehicle begins to increase dramatically. This stagnation also sends a shock wave back through the detonation products which reaches the flyer plate at about 10 μsec and causes its momentum to increase. Waves continue to reflect back and forth through the detonation products causing the momentum of both the flyer plate and the vehicle to increase continually.

The momentum predicted for the vehicle by Equation (2) is 6.22×10^6 dynes-second. We see that although the vehicle momentum is increasing steadily, it is still far short of the Equation (2) value at a time of 50 μsec. However, it has reached almost 80% of the design value of 5.0×10^6 dynes-second by this time.

The shortcoming of this analysis is that it does not take into account 2D effects, particularly venting of the detonation products. To date no studies have been done to determine how venting affects impulse generation, but it is fairly certain that it will cause a reduction.

If we assume that venting will begin when the flyer plate has moved a distance equal to its thickness, then the 1D calculation predicts that venting will occur at about 10 μsec as shown in Figure 10. If no further impulse is generated after this time, then this thruster design will generate only about 50% of the design impulse. However, this is an underestimate for two reasons.

First of all, the time for venting will actually be longer than predicted by the 1D calculations. This is because in the 1D approximation the equal flyer plate and explosive thicknesses of .080 inch give $m/c \sim 11$. Since the flyer plate extends a short distance on

either side of the charge, the actual value for m/c is about 16. This means the flyer plate will be accelerated more slowly and venting will occur later. It also means that the impulse generated by a given time will be slightly higher. These two factors combined mean that the impulse delivered to the vehicle before vent time will be somewhat higher than predicted by the 1D calculation.

Secondly, we expect some impulse to be generated after the detonation products vent. When venting occurs, although the flyer plate momentum will probably level off, the detonation products themselves will be accelerated rapidly as they become free to expand. This should give a final kick to the vehicle, although the magnitude of this kick is uncertain at present.

To assess these effects more fully, 2D calculations are required. Such calculations, both to determine the effects of venting on the impulse generation and to analyze the 2D stress environment, have been started and should be completed in the next phase of this program.

6. SUMMARY AND CONCLUSIONS

The principal problem in designing an explosive impulse generator is to achieve the desired impulse without generating an unacceptable stress environment in the vehicle. To that end we have performed a number of analyses, utilizing 1D finite difference calculations, to determine effective methods for reducing the stress environment. In addition, these same 1D calculations have been used to estimate the impulse generated by various explosive thruster systems in an effort to achieve a design that will produce the required impulse.

A variety of buffering or stress attenuation schemes were investigated involving metal foam, an air gap, and impedance mismatched layers. It was concluded that an air gap used in conjunction with impedance mismatched layers lining the cavity provides the best buffering of the systems investigated. However, additional analysis (e.g., the effect of thickness of the air gap and liners) is required to optimize this scheme.

The 1D calculations also show that it should be possible to produce the required impulse within the size constraints imposed by the overall system. However, we have shown that 2D effects are important in the impulse generation and need to be analyzed further. In particular, the effect of venting on the generation of impulse is a critical effect that should be analyzed in the future. Such a calculation for one of the systems developed here has been started and will be completed on the next phase of this program.

Although we are confident that the required impulse can be generated, at this point we do not know whether the stress environment from such a design will produce unacceptable structural damage to the vehicle. Two factors are involved in this uncertainty. First of all, this study has been limited to 1D calculations of the stress environment in order to identify promising buffering schemes. Now that a promising scheme has been identified we need to perform 2D calculations

of the stress environment. We have started such a calculation for the design shown in Figure 9; that calculation will be completed in the next phase of the program. In addition, more calculations of this type will be required as the designs are refined.

The second factor is related to our lack of understanding of the structural response of the vehicle. Although we now have at least a rough estimate of the peak stresses to be expected in the vehicle, at present we have no idea of what types of loading will produce structural damage. Large magnitude, short duration stress waves may produce damage near the cavity interface but not to other regions of the vehicle. Certain types of stress waves may produce little damage near the cavity interface but may produce spall at the inner surface of the vehicle. These are the types of phenomena that need to be analyzed.

In this study we have used titanium exclusively as the vehicle material. In another parallel study lexan was chosen for the vehicle. For a given thruster design the stress environment in titanium will be considerably higher than in lexan because of the higher shock impedance in the titanium. On the other hand, the velocity field and the strains in the lexan will be higher. Since we presently have very little understanding of the structural response of either type of vehicle to the predicted loads, there is no way to compare the results of the two studies and no quantitative way of evaluating any of the designs with respect to the stress environment produced.

To rectify this situation a series of 2D finite difference calculations of the structural response of the vehicle is required. A variety of stress histories corresponding to realistic thruster designs should be used and the response of the vehicle (including plastic flow, fracture and spall) to this loading should be calculated. Such a study will not only be useful in evaluating the designs developed thus far, but will also provide guidance in modifying those designs or in developing new ones.

As a final note, all of the analysis done thus far and planned for the future is based on 1D and 2D finite difference calculations. At

some point experimental testing of candidate designs will be required. As a preliminary step, it would be worthwhile to perform some simplified experiments in order to verify and perhaps, in a way, to calibrate the finite difference code calculations.

Code calculations such as those described in this report are useful in understanding physical processes and in making relative comparisons of various systems. They are also very useful in helping to interpret the results of experiments. However, it is a mistake to rely too heavily on these calculations for absolute predictions without the accompanying experimental verification.

REFERENCES

1. G. R. Abrahamson, "Explosively Induced Impulses," Int. Report No. 009-62, Stanford Research Institute, Menlo Park, California, July 20, 1962.

2. W. Herrmann, "Equation of State of Crushable Distended Materials," SC-RR-66-2678, Sandia Laboratory, Albuquerque, New Mexico, March 1968.

3. D. E. Maxwell, "Improved TAM Equation of State," TCAM Technical Memo 72-1, Physics International Company, San Leandro, California, 1972.

4. J. H. Tillotson, "Metallic Equations of State for Hypervelocity Impact," GA-3216, General Atomic, La Jolla, California, July 1962.

5. E. L. Lee, et al., "Adiabatic Expansion of High Explosive Detonation Products," UCRL-50422, Lawrence Radiation Laboratory*, Livermore, California, May 2, 1968.

6. "STEALTH - A Lagrange Explicit Finite-Difference Code for Solids, Structural and Thermohydraulic Analysis," Volume 1-4, EPRI NP-260, Electric Power Research Institute, Palo Alto, California, August 1976.

7. M. L. Wilkins, "Calculation of Elastic-Plastic Flow," UCRL-7322, Rev. I, Lawrence Radiation Laboratory*, Livermore, California, April 19, 1973.

8. I. G. Henry, "The Gurney Formula and Related Approximations for High-Explosive Deployment of Fragments," Report No. PUB-189, Hughes Aircraft Company, April 1967.

---

* Presently called Lawrence Livermore Laboratory

DISTRIBUTION LIST

No. of Copies	Organization
12	Commander Defense Documentation Center ATTN: DDC-DDA Cameron Station Alexandria, VA 22314
2	Director Defense Nuclear Agency ATTN: APTL RATN Washington, DC 20305
3	Director US Army Ballistic Missile Defense Advanced Technology Center ATTN: ATC-T/Mr. M. Capps ATC-M/Mr. B. Kelley ATC-M/Mr. L. Webster P. O. Box 1500 Huntsville, AL 35807
2	Commander US Army Ballistic Missile Defense Systems Command ATTN: BMDSC-HOE/Mr. Veeneman BMDSC-NW/Mr. Hurst P. O. Box 1500 Huntsville, AL 35807
1	Commander US Army Materiel Development and Readiness Command ATTN: DRCDMD-ST 5001 Eisenhower Avenue Alexandria, VA 22333
2	Commander US Army Armament Research and Development Command ATTN: DRDAR-TSS (2 cys) Dover, NJ 07801
1	Commander US Army Armament Materiel Readiness Command ATTN: DRSAR-LEP-L/Tech Lib Rock Island, IL 61299
1	Commander US Army Aviation Research and Development Command ATTN: DRSAV-E P. O. Box 209 St. Louis, MO 63166
1	Director US Army Air mobility Research and Development Laboratory Ames Research Center Moffett Field, CA 94035
1	Commander US Army Communications Research and Development Command ATTN: DRDCO-PPA-SA Fort Monmouth, NJ 07703
2	Commander US Army Harry Diamond Labs ATTN: DRXDO-TI/Tech Library DRXDO-NP/Mr. Gwaltney 2800 Powder Mill Road Adelphi, MD 20783
1	Commander US Army Electronics Research and Development Command Technical Support Activity ATTN: DELSD-L Fort Monmouth, NJ 07703
1	Commander US Army Missile Research and Development Command ATTN: DRDMI-R Redstone Arsenal, AL 35809

DISTRIBUTION LIST (cont'd)

No. of Copies — Organization

1 Commander
US Army Missile Research and Development Command
ATTN: DRDMI-YDL
Redstone Arsenal, AL 35809

1 Commander
US Army Tank Automotive Research and Development Command
ATTN: DRDTA-UL
Warren, MI 48090

1 Commander
US Army Nuclear Agency
ATTN: Mr. C. Davidson
7500 Blacklick Road
Bldg. 2073
Springfield, VA 22150

1 Director
US Army TRADOC System Analysis Activity
ATTN: ATAA-SL/Tech Library
White Sands Missile Range, NM 88002

1 Lawrence Livermore Laboratory
ATTN: D Div/Dr. Kruger
P. O. Box 808
Livermore, CA 94550

2 Los Alamos Scientific Lab
ATTN: WX-1/Dr. Charmatz
ADW/Dr. T. H. Hirons
Los Alamos, NM 87554

1 California Research and Technology, Inc.
ATTN: Mr. S. H. Schuster
6269 Variel Avenue, Suite 200
Woodland Hills, CA 91367

No. of Copies — Organization

2 Kaman Sciences Corporation
ATTN: Dr. P. Snow/Mr. Williams
Dr. P. L. Jessen
1500 Garden of the Gods Road
Colorado Springs, CO 80907

1 Martin Marietta Corporation
Orlando Division
ATTN: Mr. James Crawford
P. O. Box 5837
Orlando, FL 32805

1 Pacifica Technology
ATTN: Dr. R. T. Allen
P. O. Box 148
Del Mar, CA 92014

1 Science Applications, Inc.
ATTN: Dr. M. W. McKay
1200 Prospect Street
P. O. Box 2351
La Jolla, CA 92038

Aberdeen Proving Ground

Dir, USAMSAA
ATTN: Dr. J. Sperrazza
DRXSY-MP/H. Cohen

Cdr, USATECOM
ATTN: DRSTE- TO-F

Dir, Wpns Sys Concepts Team
Bldg E3516, Edgewood Area
ATTN: DRDAR-ACW/Mr. Olson

USER EVALUATION OF REPORT

Please take a few minutes to answer the questions below; tear out this sheet and return it to Director, US Army Ballistic Research Laboratory, ARRADCOM, ATTN: DRDAR-TSB, Aberdeen Proving Ground, Maryland 21005. Your comments will provide us with information for improving future reports.

1. BRL Report Number _____

2. Does this report satisfy a need? (Comment on purpose, related project, or other area of interest for which report will be used.)

_____

_____

_____

3. How, specifically, is the report being used? (Information source, design data or procedure, management procedure, source of ideas, etc.) _____

_____

_____

4. Has the information in this report led to any quantitative savings as far as man-hours/contract dollars saved, operating costs avoided, efficiencies achieved, etc.? If so, please elaborate.

_____

_____

5. General Comments (Indicate what you think should be changed to make this report and future reports of this type more responsive to your needs, more usable, improve readability, etc.) _____

_____

_____

_____

6. If you would like to be contacted by the personnel who prepared this report to raise specific questions or discuss the topic, please fill in the following information.

Name: _____

Telephone Number: _____

Organization Address: _____

_____

_____